Novel proton exchange membranes based on water resistant sulfonated poly[bis(benzimidazobenzisoquinolinones)]

Nanwen Li [a,b], Shenghai Li [a], Suobo Zhang [a,*], Junhua Wang [a,b]

[a] *State Key Laboratory of Polymer Physics and Chemistry, Changchun Institute of Applied Chemistry, Chinese Academy of Sciences, Changchun 130022, China*
[b] *Graduate School of Chinese Academy of Sciences, Beijing 100039, China*

ARTICLE INFO

ABSTRACT

Novel water resistant sulfonated poly[bis(benzimidazobenzisoquinolinones)] (SPBIBIs) were synthesized from 6,6′-disulfonic-4,4′-binaphthyl-1,1′,8,8′-tetracarboxylic dianhydride (SBTDA) and various aromatic ether tetraamines. The resulting polymers with IEC in the range of 2.17–2.87 mequiv g^{-1} have a combination of desired properties such as high solubility in common organic solvents, film-forming ability, and excellent thermal and mechanical properties. Flexible and tough membranes, obtained by casting from *m*-cresol solution, had tensile strength, elongation at break, and tensile modulus values in the range of 87.6–98.4 MPa, 35.8–52.8%, and 0.94–1.07 GPa. SPBIBI membranes with a high degree of sulfonation displayed high proton conductivity and a good resistance to water swelling as well. SPBIBI-b with IEC of 2.80 mequiv g^{-1} displayed the conductivity of 1.74×10^{-1} S cm^{-1} at 100 °C, which was comparable to that of Nafion® 117 (1.78×10^{-1} S cm^{-1}, at 100 °C). However, the water swelling ratio of SPBIBI-b membranes was merely 8% at 100 °C while the Nafion® 117 was 21.5%. The low swelling ratio was attributed to the strong intermolecular interaction including the electrostatic force and hydrogen bond. Moreover, they also exhibited much better hydrolytic stability than other sulfonated aromatic polymers such as polyimides. Consequently, these materials proved to be promising as proton exchange membranes.

© 2008 Elsevier B.V. All rights reserved.

1. Introduction

Sulfonated polymers have found wide applications in many industrial fields such as ion exchange resins, membrane separation, and sensors. Recently, studies on sulfonated polymers have been strongly promoted because there has been considerable interest in the development of high performance polymer electrolyte membrane fuel cells (PEMFCs) for transportation, stationary and portable power applications [1,2]. In a PEMFCs system, sulfonated polymers are used as electrolyte membrane materials for the transfer of protons from the anode to the cathode as well as for providing a barrier to the fuel gas cross-leaks between the electrodes [3]. The required properties for sulfonated polymers as a PEM materials include high ionic conductivity, good mechanical strength, dimensional stability, and high resistance to the harsh conditions of a fuel cell system [4]. Sulfonated perfluoropolymers such as Nafion® (Dupont) can satisfy many of these PEMs requirements and have found practical use in PEMFCs. However, some specific limitations exist for Nafion® membranes including their very elevated cost, high fuel permeability, and loss of the preferable properties at temperature >80 °C [5–7]. Therefore, many efforts have been expended in developing the substitutes of the perfluorinated membranes [4,8,9]. Up to now, a large number of sulfonated aromatic polymers such as, sulfonated polysulfone [10–15], sulfonated poly(ether ketone) [16,17], sulfonated poly(aryl ether) [18,19,12], and sulfonated poly(phenylene) [20,21] have been developed, and very recently sulfonated polyimides have been reported to be promising materials for PEFC [22–29]. Generally, these polymer membrane materials for PEM fuel cells rely on absorbed water and its interaction with acid groups to produce proton conductivity. To ensure high proton conductivity, high ion-exchange capacities (IECs) polymers were utilized, but these polymers swelled excessively in water (with a loss in mechanical properties) and were brittle when dry [4]. The water stability and proton conductivity of aromatic ionomers thus constitute issues that require improvement [30].

Among the non-fluorinated polymers, highly aromatic structures are preferred due to high stability. In a previous paper, we have reported that the poly[bis(benzimidazobenzisoquinolinone)] ionomers, as synthesized by sulfonated dianhydride (4,4′-binaphthyl-1,1′,8,8′-tetracarboxylic dianhydride, BTDA) and the commercially available tetraamine (3,3′-diaminobenzidine), were hydrolytically and dimensionally stable [31]. These ionomer membranes demonstrated much higher proton conductivities (10^{-2} S cm^{-1}) than sulfonated polybenzimidazoles (10^{-4} S cm^{-1})

[32], and this enhanced proton conductivity was attributed to the weakened acid–base interactions between the pyridinone ring and sulfonic acid groups due to a strong electron-withdrawing group (>C=O) substituting the H-atom in the benzimidazole ring. However, the proton conductivity for the practical application needed to be further improved. Therefore, a systematic study on the "structure-property" relationship of SPBIBIs based on different monomers is highly needed. Herein, we report the synthesis of novel SPBIBIs from SBTDA and various aromatic ether tetraamines. The effects of the structures of aromatic ether linkers on proton conducting properties, water uptake behavior, and thermal, hydrolytic, dimensional and oxidative stabilities were investigated in detail.

2. Experimental

2.1. Materials

4,4′-Binaphthyl-1,1′,8,8′-tetracarboxylic dianhydride disulfonic acid (SBTDA) was prepared according to the method previously reported [33]. Triethylamine (TEA) was dried with 4 Å molecular sieves prior to use. 3,3′,4,4′-Tetraaminodiphenyl ether was obtained by the procedure described in Ref. [34]. 1,4-Bis(3,4-aminophenoxy)phenyl, 4,4′-bis(3,4-aminophenoxy)biphenyl and 2,2′-bis[4-(3,4-diaminophenoxy)phenyl]propane were prepared as previously described [35]. All other regents were used as received without further purification.

2.2. Polymer synthesis

The typical procedure for the synthesis of SPBIBI-b is as follows: To a 100 mL completely dried 3-necked flask were charged with 0.5545 g (1 mmol) of SBTDA, 10 mL of *m*-cresol, 0.68 mL (about 2 mmol) of Et₃N, and 0.2303 g (1 mmol) 3,3′,4,4′-tetraaminodiphenyl ether successively under nitrogen flow. After the homogeneous solution was obtained, 0.2442 g (2 mmol) benzoic acid was added. The mixture was stirred at room temperature for 2 h and then heated at 80 °C for 4 h and 180 °C for 20 h. After cooling to 80 °C, additional 5 mL of *m*-cresol was added to dilute the highly viscous solution, and then the solution was poured into 200 mL acetone. The fibre-like precipitate was filtered off, washed with acetone thoroughly, and dried in vacuum oven for 12 h at 150 °C. (yield: >96%).

2.3. Membrane preparation and proton exchange

Tough, ductile ionomer membranes were prepared with a controlled thickness of 30–50 μm. The triethylamine salt form of the polymer was redissolved in *m*-cresol to form a 5–8% solution at 80 °C. This solution was filtered and cast onto glass plates at 120 °C for 12 h. Then the ionomer membrane was dried in a vacuum oven (150 °C for 24 h, 200 °C for 4 h, 250 °C for 4 h). The as-cast membrane was treated with 1.0 N sulfuric acid at room temperature for 4 days for proton exchange and the completion of proton exchange was confirmed by ^{1}H NMR measurement judging from the disappearance of the peaks corresponding to triethylamine. The proton-exchanged membrane was thoroughly washed with deionized water and then dried in vacuum at 100 °C for 10 h.

2.4. Membrane characterization

2.4.1. Measurements

^{1}H NMR spectra were measured at 300 MHz on an AV 300 spectrometer using DMSO-d_6 as solvent. FT-IR spectra were obtained with a Bio-Rad digilab Division FTS-80 FT-IR spectrometer. The inherent viscosities were determined on 0.5 g dL⁻¹ concentration of polymer in *m*-cresol with an Ubbelohde capillary viscometer at 30 ± 0.1 °C. The thermogravimetric analyses (TGAs) were obtained in nitrogen with a PerkinElmer TGA-2 thermogravimetric analyzer at a heating rate of 10 °C min⁻¹. Tensile measurement was performed with a mechanical tester Instron-1211 instrument at a speed of 1 mm min⁻¹. The samples in dry state were obtained by putting the samples in a vacuum oven at 100 °C for 10 h in vacuum and then equilibrated at 30% RH (ambient condition) for 24 h before the measurement.

2.4.2. Ion exchange capacity (IEC)

The membranes in the H⁺ form were immersed in a 1N NaCl solution for 24 h to liberate the H⁺ ions (the H⁺ ions in the membrane were replaced by Na⁺ ions). The H⁺ ions in solution were then titrated with 0.01N NaOH using phenolphthalein as an indicator.

2.4.3. Water uptake and swelling ratio

The membranes (30–40 mg per sheet) were dried at 100 °C under vacuum for 10 h until constant weight to obtain the dry material. They were then immersed into deionized water at room temperature for 4 h. After this time, the membranes were taken out, wiped with tissue paper, and quickly weighed on a microbalance. The water uptake of the membranes was calculated according to:

$$\text{water uptake} (\%) = \frac{(W_{\text{wet}} - W_{\text{dry}})}{W_{\text{dry}}} \times 100\% \tag{1}$$

where W_{dry} and W_{wet} are the weight of the dry and the corresponding water-swollen membranes, respectively.

Water Swelling Ratio of the polymer membranes were investigated by immersing the round shape samples into water at room temperature for a given time, the changes of in-plane and thickness direction were calculated from:

$$\begin{aligned} \Delta T_c &= \frac{(T - T_s)}{T_s} \\ \Delta L_c &= \frac{(L - L_s)}{L_s} \end{aligned} \tag{2}$$

where T_s and L_s are the thickness and diameter of membrane at dry state, respectively; T and L refer to those of the membrane immersed in liquid water for 5 h.

The relative swelling ratio in plane direction was calculated from:

$$\text{Relative swelling ratio} = \frac{\Delta L_c (\text{SPBBI})}{\Delta L_c (\text{Nafion}^\circledR 117)} \tag{3}$$

2.4.4. Oxidative and hydrolytic stability

Small pieces of the membrane samples with thicknesses of approximately 40 μm were soaked in Fenton's reagent (30 ppm FeSO₄ in 30% H₂O₂) at room temperature. The stability was evaluated by recording the time (τ_1) at which the membranes broke into pieces after being drastically shaken, as well as the time (τ_2) at which they dissolved completely. Furthermore, the oxidative stability was determined from changes in the weight and the reduced viscosity (η_{red}) of the test samples when the membranes broke into pieces. The hydrolytic stability was evaluated by treating the membrane samples in water at 140 °C as an accelerated testing. The proton conductivity, weight and reduced viscosity were investigated after this treatment.

2.4.5. Proton conductivity

The proton conductivity (σ, S cm⁻¹) of each membrane coupon (size: 1 cm × 4 cm) was obtained using $\sigma = d/L_s W_s R$ (d: distance between reference electrodes, and L_s and W_s are the thickness and width of the membrane, respectively). The resistance value (R) was measured over the frequency range from 100 mHz to 100 kHz by

four-point probe alternating current (ac) impedance spectroscopy using an electrode system connected with an impedance/gain-phase analyzer (Solatron 1260) and an electrochemical interface (Solatron 1287, Farnborough Hampshire, ONR, UK). The membranes were sandwiched between two pairs of gold-plate electrodes. The membranes and the electrodes were set in a Teflon cell and the distance between the reference electrodes was 1 cm. The cell was placed in a thermo-controlled chamber in liquid water for measurement. Conductivity measurements under fully hydrated conditions were carried out with the cell immersed in liquid water. All samples were equilibrated in water for at least 24 h prior to measurement. Repeated measurements were then taken at that given temperature with 10-min interval until no more change in conductivity was observed.

The relative proton conductivity was calculated from:

$$\text{Relative proton conductivity} = \frac{\sigma_{\text{SPBIBI}}}{\sigma_{\text{Nafion}^{\circledR}\,117}} \qquad (4)$$

3. Results and discussion

### 3.1. Polymers synthesis and characterization

All aromatic ether tetraamines monomers were synthesized by following the literature method [35]. With these monomers, a series of poly[bis(benzimidazobenzisoquinolinones)] were prepared by a one-step, high-temperature solution polycondensation, according to Scheme 1. The polymerizations were carried out in m-cresol in the presence of benzoic acid that acted as catalyst. The SPBIBI polymers were obtained in almost quantitative yields and displayed reduced viscosity values more than $1.32\,\text{dL}\,\text{g}^{-1}$ (Table 1). The yielded polymers in triethylamine salt form were found to be soluble in common polar aprotic organic solvents, such as DMSO, NMP, DMAc and DMF. The high solubility of all SPBIBIs may be attributed to the high degree of sulfonation (DS) and the flexible ether moieties introduced. Because the length of ether linkers in the polymer main chain is different, the obtained polymers a–e displayed ion exchange capacities (IECs) ranging from 2.87 to

2.17 mequiv g^{-1} (Table 1). Casting m-cresol solution of the polymers gave membranes with a thickness of ca. 50 μm. The obtained membranes were of deep red color with toughness and flexibility.

The polymers were characterized by ^{1}H NMR and FT-IR, and as an example, the ^{1}H NMR spectrum of the SPBIBI-e is given in Fig. 1. The peak at around 2.65 ppm was attributed to the hydrogen atom of the methyl groups. The integration ratio of this hydrogen to that of the proton in the β-position of sulfonic acid (H$_3$ and H$_4$) was close to 3:2, as expected for the composition of SPBIBI-b. No residual amide and carboxylic protons were observed. The FT-IR spectra of SPBIBI ionomer membranes are displayed in Fig. 2. Absorption bands at 1698 cm^{-1} were observed along with weak IR absorption bands at 1617 and 1548 cm^{-1}, typical of the =C=N group vibrations [36]. The former are known to be result from the characteristic stretching vibrations of the >C=O group in the pyridinone ring. Moreover, the fact that no absorption bands at 1706 and 1658 cm^{-1} which is corresponding to the C=O stretching vibration in a six-membered imide ring indicated that the title polymers were completely cyclized into pyridinone rings by the high-temperature catalytic polycondensation. The bands at 1206, 1178, and 1037 cm^{-1} were assigned to the sulfonic acid groups.

3.2. Thermal and mechanical properties

The thermal properties of SPBIBIs in proton form were assessed with TGA under a dry N$_2$ atmosphere. As shown in Fig. 3, the ionomer membranes exhibited a typical three-step degradation pattern. The first weight loss up to ca. 150 °C was ascribed to the loss of water molecules, absorbed by the highly hygroscopic −SO$_3$H groups. The second step in the range of 350–400 °C was assigned to the cleavage of sulfonic acid groups. The temperature for the second step 5% weight loss of SPBIBIs were higher than that of the sulfonated polyimides based on SBTDA (about 340 °C) [33]. The acid–base interactions between pyridinone ring and sulfonic acid groups could be responsible for the higher decomposition temperature of SPBIBIs. The last weight loss, which started around 540 °C, was attributed to the decomposition of the polymer backbone. Compared to SPBIBI-a ionomer membranes, the introduction
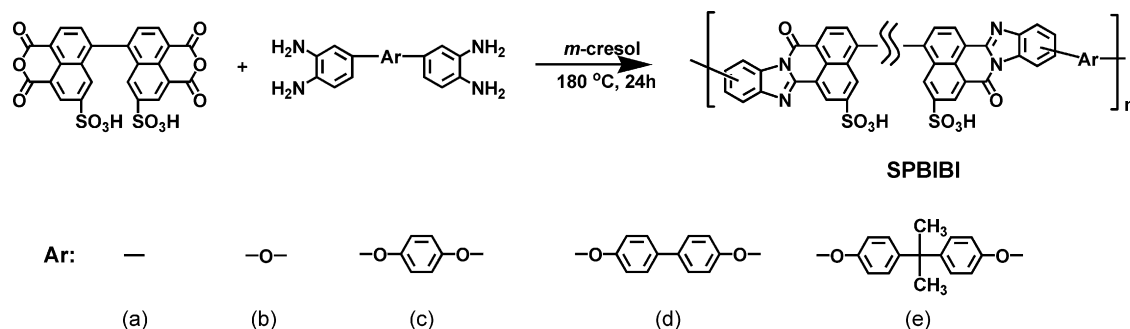
Scheme 1. Synthesis of the sulfonated poly[bis(benzimidazobenzisoquinolinones)] (SPBIBI).

Table 1
Various properties of the SPBIBI membranes.

Ionomer	η^a (dL g^{-1})	IEC (mequiv g^{-1})		Tensile strength^b (MPa)	Young's modulus (GPa)	Elongation at break (%)
		Calculated	Measured			
SPBIBI-a	1.68	2.87	2.79	98.4	1.07	35.8
SPBIBI-b	1.48	2.80	2.72	97.5	1.02	38.9
SPBIBI-c	1.55	2.49	2.34	94.3	0.95	42.8
SPBIBI-d	1.40	2.27	2.11	94.0	0.97	48.9
SPBIBI-e	1.32	2.17	2.01	87.6	0.94	64.2

^{a} 0.5 g dL^{-1} in m-cresol at 30 °C.

^{b} Samples in vacuum oven at 100 °C for 10 h in vacuum and then equilibrated at 30% RH (ambient condition) for 24 h before the measurement.
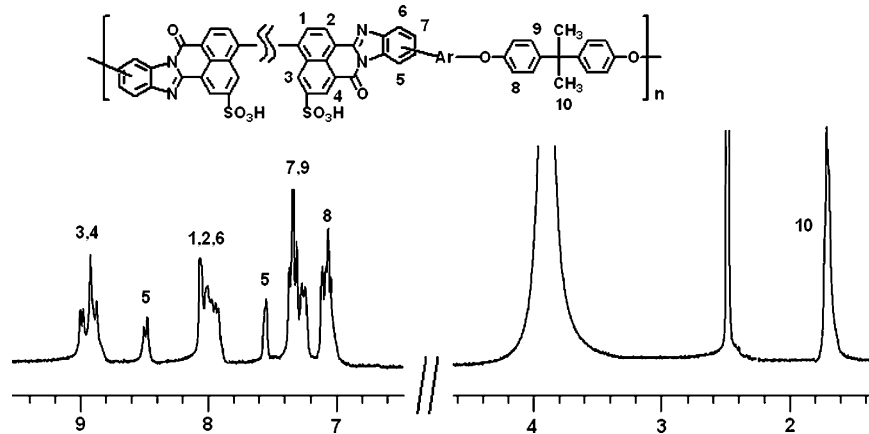
Fig. 1. An ^{1}H NMR spectrum of the SPBIBI-e material in DMSO-d_6.
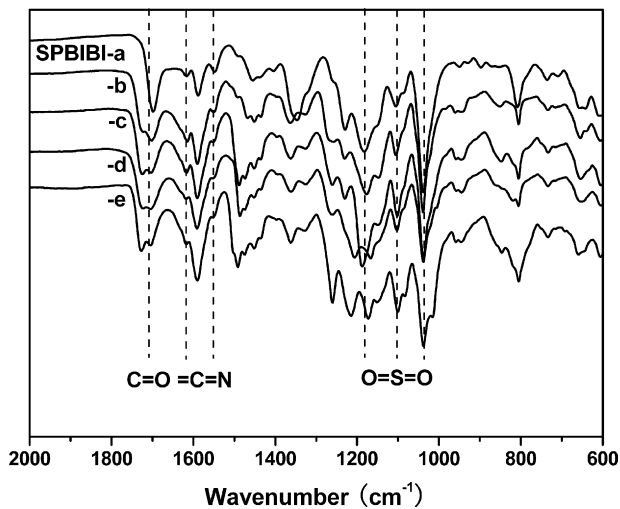

Fig. 2. FT-IR spectra of the SPBIBIs membranes.

of ether linkers was found to result in the reduction of the decomposition temperature of polymer backbone by some 100–150 °C.

The mechanical properties of the SPBIBI membranes were summarized in Table 1. The SPBIBI membranes in the dry state had
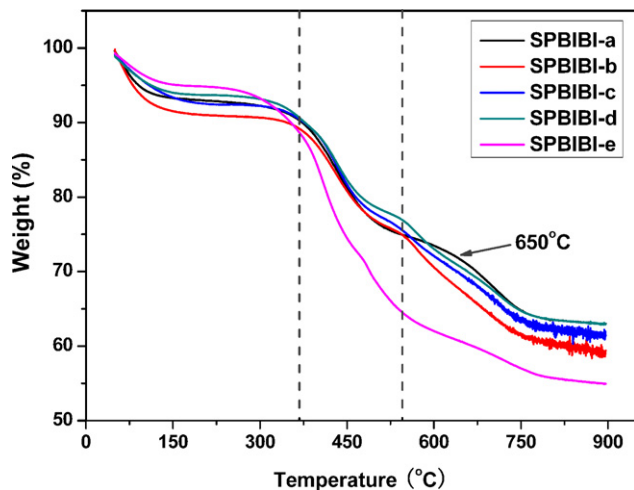
tensile stress at maximum load of 87.6–98.4 MPa, Young's moduli of 0.94–1.07 GPa, and elongations at break of 35.8–64.2%. An increase in the length of ether linkers making the polymer chain more flexible was accompanied by a decrease of tensile stress and increase of elongations at break. These results indicated that the SPBIBI membranes were strong and tough enough for fuel cell application.

3.3. Water uptake and swelling ratio

The water uptake is an important factor that directly affects proton transportation in proton conducting membranes. Generally, the water uptake (WU) of proton conducting membranes was mainly determined by IEC. In Fig. 4, the IEC dependence of the water uptake of the SPBIBIs membranes is shown. The water uptake decreased with a decreasing IEC values. At room temperature, the water uptake of the SPBIBI membranes with IECs ranging from 2.87 to 2.17 mequiv g^{-1} was in the range of 32.9–12.3%. In addition, the water uptake can also be expressed as the number of H$_2$O molecules per sulfonic acid group (λ). Each sulfonic acid group of SPBIBI membranes was solvated by less than 7 water molecules, a value much lower than that of Nafion® 117 ($\lambda = 12.1$) and other proton-conducting sulfonated aromatic polymers [4]. The lower λ value of SPBIBIs was attributed to the combination of a rigid polymer backbone and/or acid–base interactions between the pyridinone ring and the sulfonic acid groups. Compared with SPBIBI-a with comparable IEC values, SPBIBI-b membrane had lower water uptake
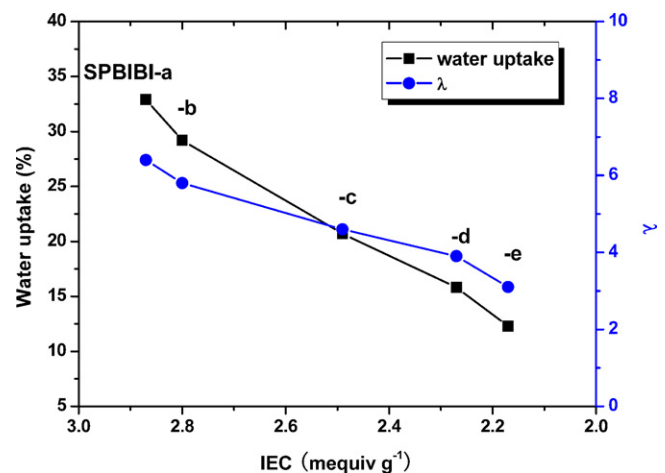

Fig. 3. TGA cures of SPBIBI membranes under dry N$_2$ atmosphere.

Fig. 4. The water uptake and λ of SPBIBI membranes as a function of IEC at 20 °C.

Table 2
The water uptake, swelling ratio and proton conductivity of the SPBIBI membranes and Nafion® 117.

Ionomer	IEC (mequiv g^{-1})	Water uptake (%)			Swelling ratio (%)				σ (mS cm^{-1})	
		20 °C	λ (20 °C)	100 °C	20 °C		100 °C		20 °C	100 °C
					Δt	Δl	Δt	Δl		
SPBIBI-a	2.87	32.9	6.4	45.5	11.2	4.0	16.2	9.0	54	125
SPBIBI-b	2.80	29.2	5.8	36.3	9.0	3.8	15.1	8.0	75	174
SPBIBI-c	2.49	20.7	4.6	26.2	8.6	3.5	14.5	6.5	34	85
SPBIBI-d	2.27	15.8	3.9	18.4	8.0	3.5	14.0	6.5	31	79
SPBIBI-e	2.17	12.3	3.1	14.2	7.6	3.3	12.1	6.2	28	72
Nafion® 117	0.90	19.6	12.1	34.5	–	11.4	–	21.5	90	178

and λ values. As shown in Table 2, the SPBIBI-b membrane showed a water uptake of 29.2% and λ values of 5.8. This was relatively low as compared to SPBIBI-a (32.9% water uptake, 6.4λ values). It was assumed that the electron-denoting ether linkers increased the basicity of tetraamines, thus the acid–base interactions. The increased acid–base interactions decreased the ability of sulfonic acid groups to form hydrogen bond with water molecules. Accordingly, the number of H_2O molecules per sulfonic acid of SPBIBI-b is less than that of SPBIBI-a counterparts.

For most proton conductive polymers, adequate water uptake is crucial for high proton conductivity. However, water swelling ratio should be also considered because extreme swelling will decrease the dimensional stability and mechanical properties of the polymer membranes. Generally, high water uptake leads to high swelling ratio. However, the structure of polymer chain also has an obvious effect on the dimensional stability. Although some of the SPBIBIs showed higher water uptake than Nafion® 117, much lower swelling ratio was observed because of the rigid polymer chain and acid–base interactions. As shown in Table 2, the SPBIBIs (a–c) membranes exhibited swelling ratios in plane direction of 3.5–4.0% at room temperature (20 °C). These were relatively low as compared to Nafion® 117 (11.4%). Fig. 5 shows the temperature dependence of water uptake and swelling ratio of SPBIBI membranes. An increase

in water uptake with increase in temperature was observed. For example, at 100 °C, SPBIBI-b in proton form showed a water uptake of 36.3% and swelling ratio in plane direction of 8%, which was only slightly higher than the corresponding values at 20 °C (29.2% water uptake and 3.8% swelling ratio in plane direction). Moreover, these membranes show unisotropic dimensional changes between in-plane and thickness directions. The SPBIBI membranes showed more than two times larger swelling ratio in thickness direction than in plane direction (Table 2). This result indicated that the SPBIBI membranes were dimensionally stable even at high temperature and humidity. The excellent dimensional stability would be preferable for an electrolyte material for PEMFC.

3.4. Proton conductivity

The proton conductivities of the SPBIBI membranes along with that of Nafion® 117 were measured in water in the temperature range of 20–100 °C, and the results are listed in Table 2. SPBIBI membranes exhibited the proton conductivities in the range of 0.31×10^{-1} to 0.75×10^{-1} S cm^{-1} at 20 °C. These were relatively low as compared to sulfonated polyimide based on SBTDA/ODA (2.78 mequiv g^{-1}, 1.61×10^{-1} S cm^{-1}, at 20 °C) and Nafion® 117 (0.90 × 10^{-1} S cm^{-1}, at 20 °C). This resulted from a strong acid–base interaction between pyridinone ring and sulfonic acid groups. Usually, the proton conductivity depended on IEC, the hydration state, and the temperature. However, the SPBIBI-a and SPBIBI-b share the same hydrophilic moieties and have the similar IEC values, differences in the proton conductivity reflect ether linkers effect on the sulfonated poly[bis(benzimidazobenzisoquinolinones)]. The SPBIBI-b membranes with flexible ether groups showed lower water uptake than SPBIBI-a membrane, but higher proton conductivity (Fig. 6). It is assumed that the flexible ether groups in the
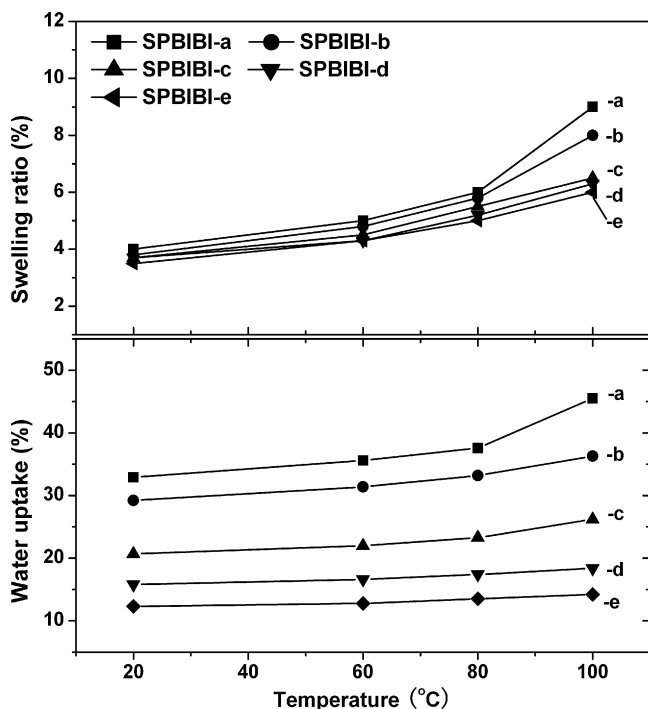

Fig. 5. Temperature dependence of the water uptake and the swelling ratio of the SPBIBI membranes.
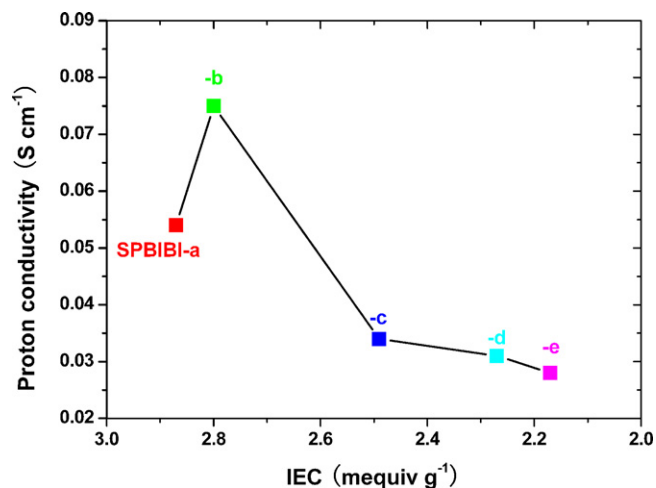

Fig. 6. The proton conductivity of SPBIBI membranes as a function of IEC at 20 °C.
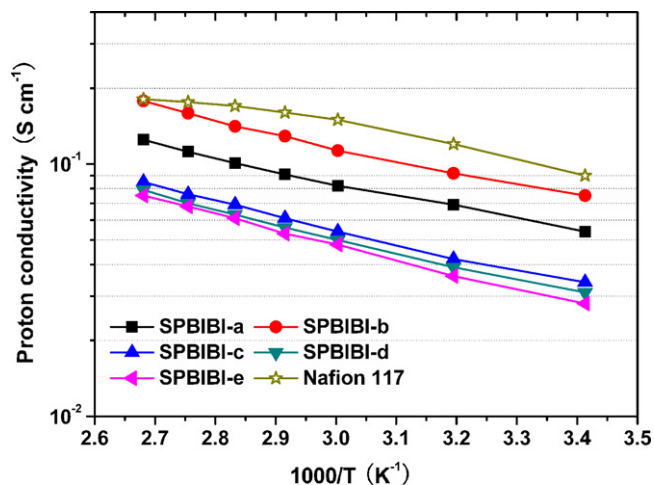
Fig. 7. Temperature dependence of the proton conductivity of SPBIBI membranes and Nafion® 117.

polymer backbone favor the water molecules diffusing through the polymer chain leading to higher proton conductivity. However, the proton conductivity was decreased when the length of ether linkers was further increased, as shown in Fig. 6. The proton conductivity of SPBIBI-e possessing lowest IEC value of 2.17 mequiv g^{-1} was 0.28×10^{-1} S cm^{-1} at 20 °C and lower by about 3 times than that of SPBIBI-b (0.75×10^{-1} S cm^{-1}, at 20 °C). This is contributed to their lower IEC values and water uptake. The temperature dependence of the proton conductivity was investigated and the results are presented in Fig. 7. All SPBIBIs membranes showed Arrhenius-type temperature dependence. At 100 °C, the SPBIBI-b membranes with high IECs of 2.80 mequiv g^{-1} showed the highest proton conductivity, i.e., 1.74×10^{-1} S cm^{-1}. This value was comparable to that of Nafion® 117 (1.78×10^{-1} S cm^{-1}). Compared to Nafion® 117, the SPBIBI-b membranes was located within the target area and thus possessed high conductivities and a low water swelling ratio, especially at high temperature (100 °C), as shown in Fig. 8.

3.5. Membrane stability toward water and oxidation

The hydrolytic stability of the SPBIBI membrane was investigated under accelerated conditions (in hot water at 140 °C for 24 h).
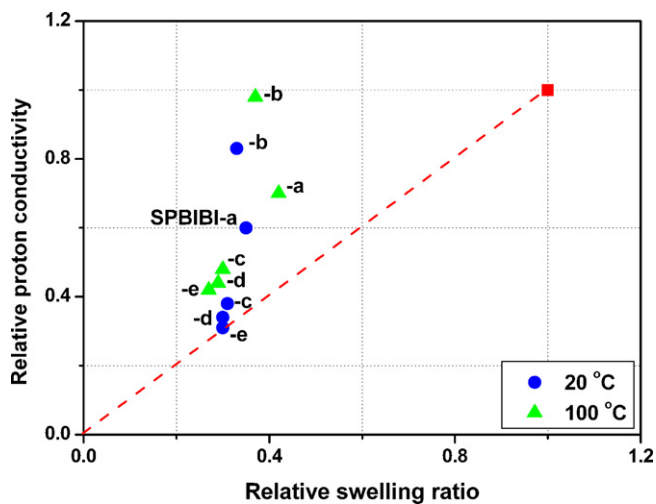

Fig. 8. Relative water swelling ratio as a function of relative proton conductivity of SPBIBI and Nafion® 117.

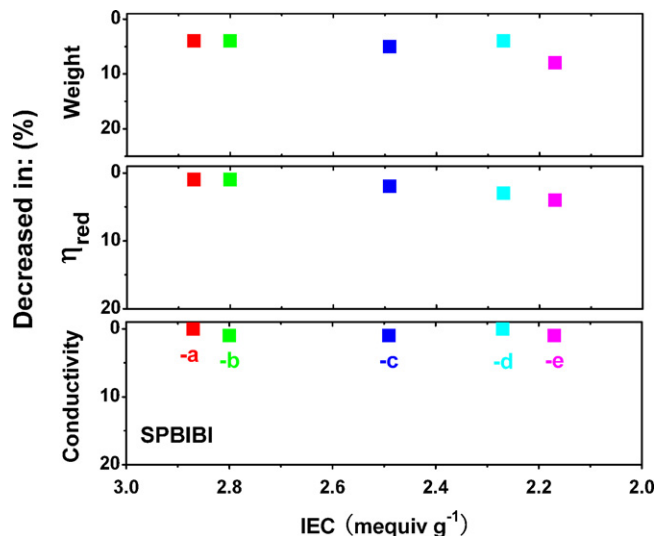**Fig. 9.** Hydrolytic stability of SPBIBI membranes as a function of IEC (measured at 140 °C in water).

After the testing, the membrane kept its flexibility and toughness without any practical changes in the weight, reduced viscosity and proton conductivity, as shown in Fig. 9. For example, the SPBIBI-e membrane did not get dissolved in hot water and experienced a weight loss of merely 8% of the weight. Moreover, there are not any virtually decreases in reduced viscosity which retained 96% of their original reduced viscosity. The results indicated that the SPBIBI membranes were hydrolytically stable.

The stability of the SPBIBI membranes to oxidation was also investigated by immersing the membranes into Fenton's reagent (30 ppm FeSO$_4$ in 30% H$_2$O$_2$) at room temperature. The oxidative stability of the samples was characterized by the elapsed time after the membranes started to dissolve (τ_1) and had dissolved completely in the solution (τ_2). Generally, the elapsed time (τ_1) increased with a decreasing IEC value because the oxidative attack by radical species should mainly occur in or in the proximity of water-containing hydrophilic domains. Thus, the SPBIBI-e membrane with the lowest IEC values (2.17 mequiv g^{-1}) displayed best oxidation stability as compared to that of other SPBIBI membranes. As shown in Table 3, the elapsed time (τ_1) for SPBIBI-e membranes was 18 h and 25 h were required before the pieces had become completely dissolved. However, the SPBIBI-a possessing highest IEC values (2.87 mequiv g^{-1}) exhibited a comparable stability ($\tau_1 = 18$ h, $\tau_2 = 22$ h) to that of the SPBIBI-e membrane. It is considered that the oxidative attacked by radicals are electrophilic and occur most likely on the main chain aromatic rings bound with electron-donating ether groups. The SPBIBI-a possesses the wholly aromatic polymer chain structures, thus the excellent oxidative stability.

Table 3
The oxidative stability of various SPBIBI membranes.

Ionomer	IEC (mequiv g^{-1})	Oxidative stability[a]	
		τ_1[b] (h)	τ_2[c] (h)
SPBIBI-a	2.87	18	22
SPBIBI-b	2.80	14	23
SPBIBI-c	2.49	15	23
SPBIBI-d	2.27	17	24
SPBIBI-e	2.17	18	25

[a] 30 °C in 30% H$_2$O$_2$ containing 30 ppm FeSO$_4$ at room temperature.
[b] The time when the membrane broke into pieces after being shaken drastically.
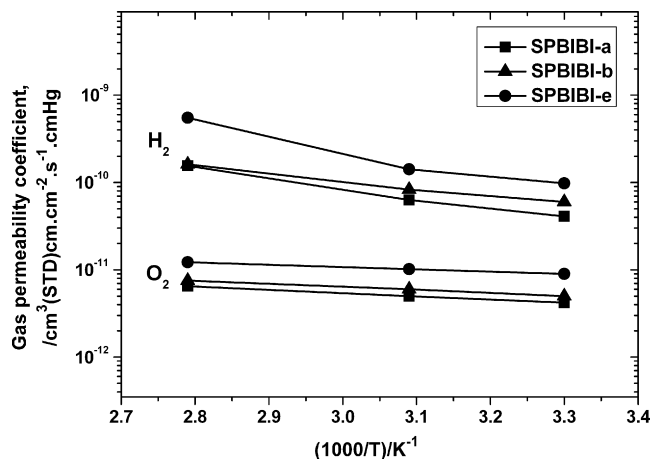[c] The time when the membrane dissolved completely.

Fig. 10. Temperature dependence of the dry hydrogen and oxygen permeability of SPBIBI-a, SPBIBI-b and SPBIBI-e membranes.

3.6. Gas permeability

Gas permeability through the proton exchange membrane is an important factor that affects fuel cell performance, because the permeated gas causes direct chemical reaction combustion resulting in lower utilization of fuels and higher overpotential, particularly at the cathode reaction. Hydrogen and oxygen permeability coefficients for typical SPBIBI membrane under dry condition are summarized in Fig. 10 as a function of temperature. All the SPBIBI ionomer membranes were much less permeable to both gases than Nafion®. In the range of tested temperature, dry hydrogen and oxygen permeabilities of SPBIBI membrane more than 2 orders of magnitude lower than those of Nafion® [14]. Higher IEC membranes (SPBIBI-a) resulted in lower gas permeability since gases permeate mainly through hydrophobic domain of ionomer membranes [37].

4. Conclusions

A series of novel water resistant sulfonated poly[bis(benzimidazobenzisoquinolinones)] were synthesized by high temperature condensation from 6,6′-disulfonic-4,4′-binaphthyl-1,1′,8,8′-tetracarboxylic dianhydride (SBTDA) and various aromatic ether tetraamines as proton exchange membranes. The obtained polymers exhibited excellent film-forming ability and mechanical properties. These SPBIBI membranes displayed excellent dimensional stability because of the rigid polymer chain and acid–base interactions between pyridinone ring and sulfonic acid groups. Moreover, the SPBIBI membranes exhibited excellent thermal and hydrolytic stabilities. They retained unchanged with regard to weight, reduce viscosity and proton conductivity after 24 h of hydrolytic testing in water at 140 °C. At 100 °C, the SPBIBI-b membranes possessing an ether group showed the proton conductivity, i.e. 1.74×10^{-1} S cm^{-1}. This value was comparable to that of Nafion® 117 (1.78×10^{-1} S cm^{-1}), but higher than that of SPBIBI-a counterparts without any flexible ether groups (1.25×10^{-1} S cm^{-1}). It is assumed that the flexible ether groups of SPBIBI-b favor the water molecules diffusing through the polymer chain. The present results indicated that these SPBIBI membranes can be considered as promising polymer ionomers for PEMFC applications.

References

[1] K.D. Kreuer, J. Membr. Sci. 185 (2001) 29–39.
[2] B.C.H. Steele, A. Heinzel, Nature (London) 414 (2001) 345–352.
[3] L. Carrette, K.A. Friedrich, U. Stimming, Fuel Cells 1 (2001) 5–39.
[4] M.A. Hickner, H. Ghassem, Y.S. Kim, B.R. Einsla, J.E. McGrath, Chem. Rev. 104 (2004) 4587–4611.
[5] K.A. Mauritz, R.B. Moore, Chem. Rev. 104 (2004) 4535–4586.
[6] Y.S. Kim, L. Dong, M.A. Hickner, T.E. Glass, V. Webb, J.E. McGrath, Macromolecules 36 (2003) 6281–6285.
[7] O. Savadogo, J. Power Sources 127 (2004) 135–161.
[8] K. Rikukawa, K. Sanui, Prog. Polym. Sci. 25 (2000) 1463–1502.
[9] Q. Li, R. He, J.O. Jensen, N.J. Bjerrum, Chem. Mater. 15 (2003) 4896–4915.
[10] J.A. Kerres, J. Membr. Sci. 185 (2001) 3–27.
[11] D.S. Kim, K.H. Shin, H.B. Park, Y.S. Chung, S.Y. Nam, Y.M. Lee, J. Membr. Sci. 278 (2006) 428–436.
[12] K. Miyatake, Y. Chikashige, M. Watanabe, Macromolecules 36 (2003) 9691–9693.
[13] K.B. Willes, F. Wang, J.E. McGrath, J. Polym. Sci. Part A: Polym. Chem. 43 (2005) 2964–2976.
[14] K. Miyatake, Y. Chikashige, E. Higuchi, M. Watanabe, J. Am. Chem. Soc. 129 (2007) 3879–3887.
[15] D.S. Kim, G.P. Robertson, M.D. Guiver, Macromolecules 41 (2008) 2126–2134.
[16] P. Xing, G.P. Robertson, M.D. Guiver, S.D. Mikhailenko, K. Wang, S. Kaliaguine, J. Membr. Sci. 229 (2004) 95–106.
[17] S. Matsumura, A.R. Hlil, C. Lepiller, J. Gaudet, D. Guay, Z. Shi, S. Holdcroft, A.S. Hay, Macromolecules 41 (2008) 281–284.
[18] L. Wang, Y.Z. Meng, S.J. Wang, X.Y. Shang, L. Li, A.S. Hay, Macromolecules 37 (2004) 3151–3158.
[19] K. Miyatake, K. Oyaizu, E. Tsuchida, A.S. Hay, Macromolecules 34 (2001) 2065–2071.
[20] H. Ghassemi, J.E. McGrath, Polymer 45 (2004) 5847–5854.
[21] S. Wu, Z. Qiu, S. Zhang, X. Yang, F. Yang, Z. Li, Polymer 47 (2006) 6993–7000.
[22] C. Genies, R. Mercier, B. Sillion, N. Cornet, G. Gebel, M. Pineri, Polymer 42 (2001) 359–373.
[23] X. Guo, J. Fang, T. Watari, K. Tanaka, H. Kita, K.I. Okamoto, Macromolecules 35 (2002) 6707–6713.
[24] K. Miyatake, H. Zhou, H. Uchida, M. Watanabe, Chem. Commun. (2003) 368–369.
[25] K. Miyatake, H. Zhou, M. Watanabe, Macromolecules 37 (2004) 4956–4960.
[26] B.R. Einsla, Y. Hong, Y.S. Kim, F. Wang, N. Gunduz, J.E. McGrath, J. Polym. Sci. Part A: Polym. Chem. 42 (2004) 862–874.
[27] X.B. Chen, Y. Yin, P. Chen, H. Kita, K.I. Okamoto, J. Membr. Sci. 313 (2008) 106–119.
[28] Y. Yin, O. Yamada, K. Tanaka, K.I. Okamoto, Polymer. J. 38 (2006) 197–219.
[29] K. Miyatake, Y. Tomohiro, M. Watanabe, J. Polym. Sci. Part A: Polym. Chem. 46 (2008) 4469–4478.
[30] R. Borup, J. Meyers, B. Pivovar, Y.S. Kim, R. Mukundan, N. Garland, D. Myers, M. Wilson, F. Garzon, D. Wood, P. Zelenay, K. More, K. Stroh, T. Zawodzinski, J. Boncella, J.E. McGrath, M. Inaba, K. Miyatake, M. Hori, K. Ota, Z. Ogumi, S. Miyata, A. Nishikata, Z. Siroma, Y. Uchimoto, K. Yasuda, K.I. Kimijima, N. Iwashita, Chem. Rev. 107 (2007) 3904–3951.
[31] N. Li, S. Zhang, J. Liu, F. Zhang, Macromolecules 41 (2008) 4165–4172.
[32] J. Jouanneau, R. Mercier, L. Gonon, G. Gebel, Macromolecules 40 (2007) 983–990.
[33] N. Li, Z. Cui, S. Zhang, S. Li, J. Polym. Sci. Part A: Polym. Chem. 46 (2008) 2820–2832.
[34] V.L. Bell, R.A. Jewell, J. Polym. Sci. Part A-1 5 (1967) 3043–3060.
[35] J. Wang, N. Li, F. Zhang, S. Zhang, J. Liu, submitted for publication.
[36] Z.J. Jedlinski, B. Kowalski, U. Gaik, Macromolecules 16 (1983) 522–526.
[37] F. Piroux, E. Espuche, R. Mercier, J. Membr. Sci. 232 (2004) 115–122.